An enantiopure propeller-like trityl-brominated radical: Bringing together a high racemization barrier and an efficient circularly polarized luminescent magnetic emitter

Paula Mayorga-Burrezo,[†[a]] Vicente G. Jiménez,[†[b]] Davide Blasi,[†[a]] Teodor Parella,[[c]] Imma Ratera,*[[a]] Araceli G. Campaña*[[b]] and Jaume Veciana.*[[a]]

[a] Dr. P. Mayorga-Burrezo, Dr. D. Blasi, Dr. I. Ratera, Prof. J. Veciana
Department of Molecular Nanoscience and Organic Materials
Institut de Ciència de Materials de Barcelona (ICMAB)/ CIBER-BBN
Campus Universitari de Bellaterra. E-08193, Cerdanyola, Barcelona, Spain.
E-mail: vecianaj@icmab.es; iratera@icmab.es

[b] V. G. Jiménez, Dr. A. G. Campaña
Department of Organic Chemistry,
University of Granada (UGR)
C. U. Fuentenueva, 18071 Granada, Spain.
E-mail: araceligc@ugr.es

[c] T. Parella
Servei de Ressonancia Magnetica Nuclear
Universitat Autonoma de Barcelona. Campus Universitari de Bellaterra. E-08193, Cerdanyola, Barcelona, Spain.

† Equally contributed to this work

Supporting information for this article is given via a link at the end of the document.

Abstract: A new persistent organic free radical has been synthetized with Br atoms occupying the *ortho*– and *para*– positions of a trityl core. After the isolation of its two propeller-like atropisomers, Plus *(P)* and Minus (*M*), their absolute configurations were assigned by a combination of theoretical and experimental data. Remarkably, no hints of racemization were observed up to 60 °C for more than two hours, due to the higher steric hindrance imposed by the bulky Br atoms. Therefore, when compared to its chlorinated homologue ($t_{1/2}$ = 18 s at 60 °C), an outstanding stability against racemization was achieved. Circularly polarized luminescence (CPL) response of both enantiomers was detected. This free radical shows a satisfactory luminescent dissymmetry factor ($|g_{lum}(592\ nm)| \approx 0.7 \times 10^{-3}$) despite its pure organic nature and low luminescence quantum yield (LQY). Improved organic magnetic CPL emitters derived from the reported structure can be envisaged thanks to the wide possibilities that Br atoms at *para*-positions offer for further functionalization.

Introduction

Nowadays, the use of organic radicals in optics and optoelectronics is capturing increasing interest. The reason behind is the highly efficient photoluminiscence arising from their open-shell electronic configuration. In fact, in these kind of compounds, the emission comes from the spin-allowed radiative decay of doublet excitons, avoiding the common fluorescence quenching related to non-doublet excited states.[1,2] Among the organic emitters with unpaired electrons, particular attention has been devoted to triphenylmethyl (trityl) radical-based chlorinated derivatives.[3] In addition to their remarkable persistence and chemical stability, they also present: *(i)* high values of luminescence quantum yield (LQY) at long wavelengths, especially when dispersed in rigid hosts;[4-6] and *(ii)* non-linear optical activity,[7] such as high two-photon absorption (2PA) cross-sections.[8] Even though they were first reported several decades ago, they are, indeed, far to be an extinct research field. In this sense, different synthetic approaches are currently being pursued aiming to obtain higher photostability and LQY values or red-shifted emissions.[9-15] In addition, cutting-edge devices have recently been developed based on these singular open-shell structures.[16]

Following this trend, some of us addressed the first report of organic free radicals as circularly polarized luminescence (CPL) emitters in a previous work.[17] For such a purpose, enantiomers of tris(2,4,6-trichlorophenyl)methyl[18] and perchlorotriphenylmethyl[19] radicals (**TTM** and **PTM** radicals, respectively in Figure 1) were separated and studied. Their intrinsic chirality as molecular propellers[20] and, most of all, the influence on their emissive properties were reported. In that context, opposite signed CPL responses were detected for each pair of enantiomers. Their luminescence dissymmetry factors ($|g_{lum}(\lambda)|$) were also determined, considering the left- and right-handed circularly polarized light intensities (i.e., $I_L(\lambda)$ and $I_R(\lambda)$, respectively) emitted by both isomers at a given wavelength (λ), according to $[I_L(\lambda)-I_R(\lambda)]/\cdot[I_L(\lambda)+I_R(\lambda)]$. Those $|g_{lum}(\lambda)|$ values were also compared with their respective absorption anisotropy factors or $|g_{abs}(\lambda)|$,[21] at the longest wavelength, measured by electronic circular dichroism (ECD). In that case, the differential absorption of the left- and right-handed circularly polarized light in terms of molar absorptivities (ε) were considered, according to $[\varepsilon_L(\lambda)-\varepsilon_R(\lambda)]/\cdot[\varepsilon_L(\lambda)+\varepsilon_R(\lambda)]$. As a result, efficient chiral emissions for both samples were set, since $|g_{abs}(\lambda)|/|g_{lum}(\lambda)|$ ratios close to unity[22] were obtained. Full stability against racemization of the two possible enantiomers, Plus *(P)* and Minus *(M)*, was proved at the selected working conditions (*i.e.*: -20 °C in viscous CCl_4 solutions).

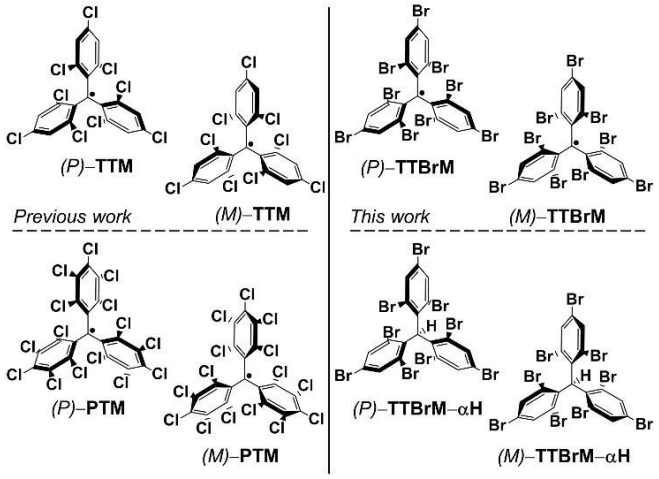

Figure 1 Left: Chemical structures of the propeller-shaped **TTM** radical (top) and **PTM** radical (bottom), first organic free radicals studied as CPL emitters in a previous work.[17] Right: Chemical structure of the newly synthetized trityl-based **TTBrM** radical (top) together with its non-radical counterpart **TTBrM–αH** (bottom). In all cases, atropisomers *Plus* (*P*-) and *Minus* (*M*-) are depicted.

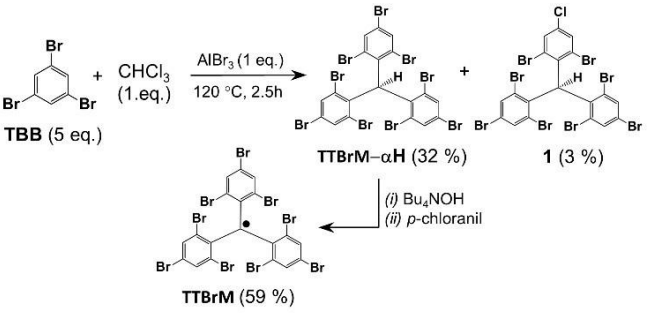

Scheme 1. Synthetic route for **TTBrM** radical, with compound **1** as a by-product of the Friedel-Crafts reaction. Since racemic mixtures of the atropisomers were obtained for both compounds, no conformations are depicted.

However, partial racemization was detected at additional working conditions at room temperature, confirming the inability of the Cl atoms of **TTM** and **PTM** radicals to completely suppress the racemization. Aiming to sort this issue out, the replacement of Cl substituents by more voluminous substituents, like Br, was thought. Taking into account that a higher steric hindrance should result in a high rotation energy barrier of phenyl rings, the racemization at room temperature may be avoided.

Herein, we present the newly synthesized tris(2,4,6-tribromophenyl)methyl radical (named as **TTBrM** in Figure 1), with Br atoms at the *ortho*– and *para*– positions. With this new radical compound a step further in order to complete the series of halogenated trityl compounds has been achieved since chlorine (**TTM**) and fluorine derivatives[23,24] had already been reported. The stereochemistry of this new bromide derivative has been evaluated gaining deeper insights into its racemization kinetics after the inclusion of the bulky bromine atoms. Finally, CPL activity has been considered. Overall, a higher conformational stability has been proved, leading to a more efficient fully organic CPL radical emitter.

Results and Discussion

Synthesis and structural characterization

TTBrM-αH, the precursor of **TTBrM** radical, was obtained by a Friedel-Crafts reaction using an excess of 1,3,5-tribromobenzene (**TTB**) and $CHCl_3$ (or $CHBr_3$), as alkylating agent, with $AlCl_3$ (or $AlBr_3$) as catalyst. (See Section S1 of the Supporting Information (SI) for further details about the synthesis and chemical characterizations). The highest yield of **TTBrM-αH** with the lowest amount of the by-product **1** were attained with the conditions summarized in Scheme 1. Pure **TTBrM–αH** was then treated with tetrabutylammonium hydroxide. Then, a subsequent oxidation of the resulting anion with *p*–chloranil[18] was performed, giving to **TTBrM** radical.

Crystallization of the resulting racemic mixtures of **TTBrM** radical and **TTBrM–αH** derivative was faced by slow diffusion in a CH_2Cl_2/Hex (1:1) mixture at room temperature (Section S2 of SI file). X-Ray diffraction data from the obtained single crystals revealed the presence of two propeller-shaped enantiomers, *Plus* (*P*) and *Minus* (*M*), for both compounds (Figure 1 and Fig. S11). In addition, such data showed considerable dissimilarities between the molecular structures of the radical and non-radical counterpart, mainly due to the different hybridization (*i.e., sp*^{2} *vs sp*^{3}, respectively) of their α-carbon atoms (Fig. S12 and Table S1). A worth noticing point is the crystal and molecular structures of **TTBrM** radical and its comparison with the chlorinated version, **TTM** radical. Both radicals crystallize in the same space group, C2/*c*. They also exhibit the same tilt angles (i.e., $\varphi \sim 47°$) of the three phenyl rings with respect to the plane of the central C atoms (formed by the α- and *ipso*-carbons), related to the repulsion among the halogen atoms in *ortho*– positions. Thereby, both molecules adopt a chiral propeller-like conformation with three halogens above the plane of the central C atoms and three others under this plane, despite the remarkable difference on the van der Waals radius of its halogen substituents (185 *vs*. 175 pm for Br and Cl atoms, respectively). Consequently, the higher repulsion among the Br atoms, due to its larger size, is relaxed by stretching the bonds between the α- and the *ipso*-carbons becoming 1.482 Å for **TTBrM** radical versus 1.461 Å for **TTM** radical. In this sense, the bulkier Br atoms do not change the torsions of the rings but enlarge the bonds of the phenyl rings with the central C atoms. This resulted in a slightly decreasing of the delocalization of the unpaired electron onto the rings, which affects somewhat the optical properties (*vide infra*).

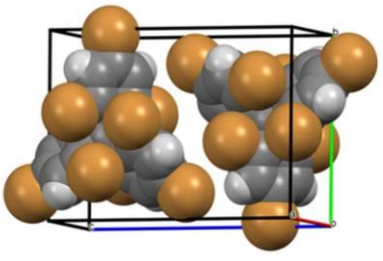

Figure 2. Space-filing representation of *Plus* (left) and *Minus* (right) enantiomers of **TTBrM** radical observed in the X-ray crystal structure.

Optical properties

As depicted in Figure 3 (top), the UV-Vis electronic absorption spectrum of **TTBrM** radical shows the corresponding features of the so-called C and D bands of trityl derivatives,[25] at 400 nm (ε = 26797 cm^{-1} M^{-1}) and 565 nm (ε = 1070 cm^{-1} M^{-1}) respectively, ascribed to the delocalization of the unpaired electron through the aromatic rings (see more details in Section S3 from SI file). Compared to the values for the C/D bands reported for **TTM** radical at the same experimental conditions (C band: 380 nm and D band: 460/500/545),[17] a red-shift resulted for the bromine substituted derivative.

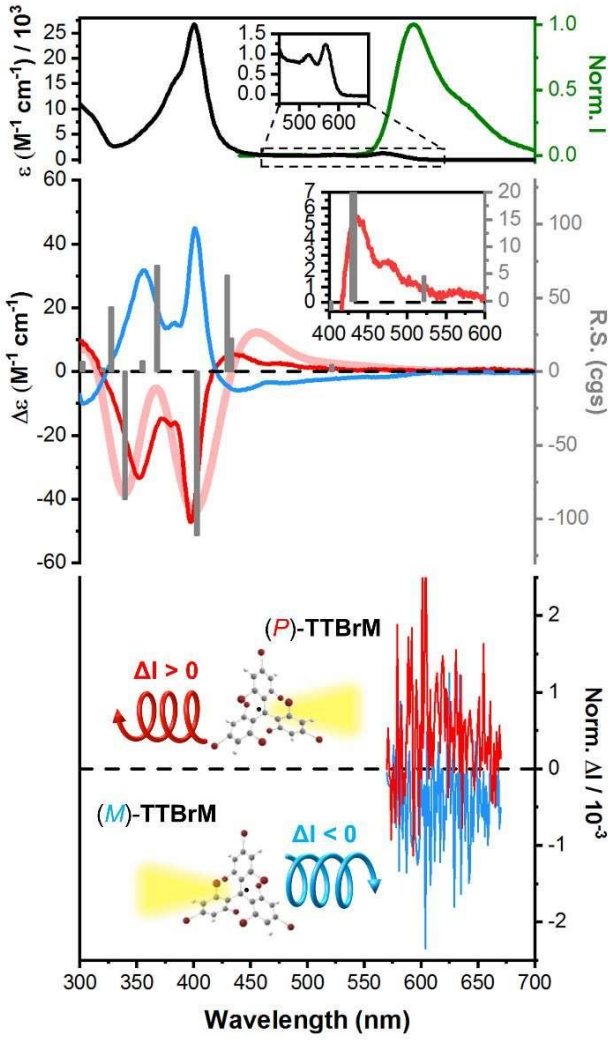

Figure 3. Top: Experimental UV-Vis absorption spectra (~10^{-4} M in CCl_4 at - 18 °C, in black) of **TTBrM,** together with the total fluorescence spectra (~10^{-5} M in CCl_4, at -18 °C, in green). Inset: Experimental UV-Vis absorption D band (See Fig. S29 of SI for theoretical UV-Vis absorption spectra). Central: Experimental ECD spectra (10^{-4} M in CCl_4 at -18 °C) of the first (blue) and second (red) (CSP)HPLC eluted fractions together with the calculated ECD spectra of (*P*)-**TTBrM** (thick light red line). The sticks (dark grey) indicate the positions and rotatory strengths of the TD-DFT calculated transitions. Inset: Experimental (~10^{-4} M in CCl_4 at -18 °C) and theoretical ECD D band for the second (red) (CSP)HPLC fraction. Bottom: CPL spectra of the two (CSP)HPLC fractions of **TTBrM** (10^{-4} M in CCl_4 at -18 °C), collected with λ_{exc} set to UV-Vis C band. Additionally, a schematic representation of the CPL response of the two enantiomers has been included, with ΔI > 0 and ΔI < 0 for (*P*)- and (*M*)-enantiomers, respectively.

Regarding the luminescence properties, a red fluorescence emission centered at 593 nm and extended up to 750 nm was detected for **TTBrM** radical when irradiated with UV light. Excitation independent emission and overlapping between absorption and excitation spectra were observed. The Stokes shift was also evaluated (Fig. S15 of SI file), considering the longest-wavelength absorption (D band). A higher value than the one for the chlorinated derivative was found (*i.e.,* **TTM** radical: 774 cm^{-1} and **TTBrM** radical: 836 cm^{-1}). Consequently, a smaller loss of photon energy than in **TTM** radical may occur during the transition of **TTBrM** radical to its ground state, despite its probed higher robustness.

When facing the evaluation of the LQY, the excitation wavelength (i.e., λ_{exc}) was fixed at the wavelength of the maximum absorption of the C band, aiming to reach a higher value,[26] since no further derived changes in the emission spectrum were expected.[27] Thus, a LQY of 1.8% in viscous CCl_4 at -18 °C was achieved. This low value was attributed to the absence of a complete rigid media, analogously to the case of **TTM** radical (LQY: 7.2% in CCl_4 at - 20 °C). Moreover, the less electron withdrawing effect of Br atoms might be behind such a lower yield in comparison with the **TTM** one. In fact, similar LQY were observed by Hattori *et al*.[28] when performing a partially substitution of the *ortho*– positions in one ring of **TTM** radical with bromine atoms, underlining the importance of the halogens in determining the optical properties.

Resolution and Evaluation of the Racemization Barrier

The racemic resolution of **TTBrM** radical into its two enantiomers (i.e., *Plus (P)* and *Minus (M),* (Figure 1)[29] was faced by chiral stationary phase chromatography (CSP) HPLC, using a cellulose-based stationary phase. In agreement with the previously described conditions for **TTM** radical, a 99.9:0.1 (v/v) Hex/CH_2Cl_2 mixture as eluent was used, under isocratic conditions at room temperature.[16] According to what was expected, a complete enantiomeric separation was achieved (Fig. S17) and larger retention times were observed when compared with the chlorinated radical version (i.e., 12.4 / 18.6 min for **TTBrM** radical and 5.65 / 6.49 min for **TTM** radical).

Variable-temperature ECD, also known as dynamic ECD (i.e., dECD) technique was chosen for evaluating the stability of the enantiomers in solution, since some overestimated thermodynamic data might be obtained from the analysis of the elution profiles resulting from the dynamic (CSP)HPLC method.[30] The evolution with time of the ECD signal of the second eluted (CSP)HPLC fraction was recorded at different temperatures in order to quantify the kinetic parameters of the enantiomerization barriers. Interestingly, no hints of racemization were observed at any temperature up to 60 °C for the **TTBrM** radical (see Section S5 of SI file), in contrast to the previously observed behaviour for the **TTM** radical, with a $t_{1/2}$ of 18 s at that given temperature. According to this, the supremacy of the brominated derivative over the chlorinated one in terms of thermal stability is worth of mention. In order to get further insight into the effect of the Br atoms, 1D NOESY/EXSY 1H NMR measurements[31] were also carried out for the non-radical **TTBrM–αH** derivative, taking full advantage of its closed shell configuration. In analogy with previous results, no chemical exchange was observed up to 110 °C while, conversely, almost 1:1 racemate was detected for the homologue **TTM–αH** derivative at 90 °C (see Section S6 of the SI file). Hence, the replacement of Cl atoms by Br ones in both (radical and αH)

compounds results into a large enhancement of their racemization barriers leading to more robust chiral derivatives. In this sense, one of the main targets of this research was successfully achieved.

Chiroptical properties

Figure 3 (central) shows the monitored ECD response of the two collected enantiomeric (CSP)HPLC eluted fractions for **TTBrM** radical. The main spectroscopic features are: *(i)* an excellent signal-to-noise ratio; *(ii)* limited baseline drift, even at shorter wavelengths; *(iii)* nearly perfect mirror-imaged Cotton effects; and *(iv)* great alignment with the corresponding UV-Vis spectrum measured by conventional spectroscopy. In fact, corresponding features to the C and D UV-Vis electronic absorption bands were found in both ECD spectra. Their $|g_{abs}(\lambda)|$ were also estimated at -18 °C, in order to be consistent with further experiments: $|g_{abs}$(C ECD band)$|= 1.6\cdot10^{-3}$ and $|g_{abs}$(D ECD band)$|= 1.5\cdot10^{-3}$, respectively (see Section S7 of SI file). As occurred in the case of **TTM** radical, the D ECD band resulted to have opposite Cotton effects to that of the main feature of the spectrum (*i.e.,* C ECD band). According to literature, the sign of minor absorption bands at longest wavelengths can play a relevant role, since they usually determine the sign of the CPL spectrum,[32] as occurs for the case of carbo[n]helicenes.[33] Thus, in line with previous results,[17] *(P)*–**TTBrM** radical was associated with the second eluted (CSP)HPLC fraction while the first one, with a (-) 567 nm ECD D band, was related to the *(M)*–**TTBrM** radical. Unfortunately, no enantiopure monocrystals for X-ray diffraction could be obtained to assign the Absolute Configuration (i.e*.,* AC) of the (*P*)- and (*M*)-enantiomers. Conversely, a comparison between experimental ECD spectra with data from TD-DFT calculations[34] was done. Figure 3 (central) portrays the calculated UB3LYP/6-311+G** ECD spectrum for *(P)*–**TTBrM** radical, showing a reasonably good agreement found with the experimental ECD of the second eluted (CSP)HPLC fraction (see Section S8 of SI file for further details). Actually, a positive Cotton effect for the lowest-energy transition, i.e., D band, was theoretically obtained (see inset in Figure 3 (central)), corroborating the AC assignment.

Encouraged by the high photostability of **TTBrM** radical with a half-life ($t_{1/2}$) of 4.58 x 10^4s (Fig. S16 of SI file) together with the revealing CPL response of **TTM** radical,[17] CPL was also evaluated for the two enantiomers of **TTBrM** radical. As previously illustrated with the enantiomers of **TTM** radical, the following issues were envisaged: *(i)* good CPL signals are only reached when both, large $|g_{lum}(\lambda)|$ and LQY values, are achieved;[35] *(ii)* drastically enhancement of the LQY occurs when these molecules are confined in a rigid host;[36] but *(iii)* solid media as frozen glasses are considered as birefringent elements since they can produce optical artefacts.[37] Thus, same homogenous viscous media (i.e., CCl_4 solutions at -18 °C) was used for this study, where no excimeric bands[36] were found thanks to a good solvation. In line with ECD results, identical emission spectra were recorded for the enantioenriched and racemic solutions.

¡Error! No se encuentra el origen de la referencia.(bottom) depicts the CPL spectra of the two enantiomers recorded after the deoxygenation of the enantioenriched solutions. In this sense, due to the brominated substitution, the photodegradation of the radical compound once in the excited state was minimized and up to 100 scans (in the 570 – 670 nm range) could be averaged in order to obtain clearer CPL signals. Corroborating the AC assignment, opposite signed CPL activity was obtained, as expected for a pure CPL response. A good agreement with the signs of their respective Cotton effects of D bands in ECD spectra were also achieved. (See Section S9 of the SI file for further details, including a comparison with the CPL activity obtained for the racemic mixture, as well as a statistical analysis of all the acquired data). The $|g_{lum}(\lambda)|$ for **TTBrM** radical was estimated to be (x 10^{-3}): ≈ 0.7 (Fig. S32-33 of SI file), lower than its previously calculated $|g_{abs}$(D ECD band)$|$ (x 10^{-3}): ≈ 1.52 value. However, compared with the recently reported $|g_{lum}$(D ECD band)$| = 0.5\cdot10^{-3}$ factor for **TTM** radical,[17] it is safe to say that a more efficient chiroptical response has been achieved with this new organic radical. Thus, the second main target of this research was also achieved.

Conclusion

A new brominated trityl derivative, namely **TTBrM** radical, has been successfully developed as a persistent and highly efficient organic free radical CPL emitter. Compared to the already reported data for its chlorinated homologue, an outstanding enhancement in the racemization barrier has been achieved. Moreover, since an easy functionalization of the trityl core can be carried out, taking into account the easier leaving capacity of the Br atoms at the para positions, **TTBrM** radical might be considered as the starting point of a new family of trityl radical derivatives and a new research field. In this sense, with improved organic free radicals combining chiral, magnetic and luminescent properties as required, future devices are a step closer from this moment on.

Experimental Section

Synthesis and X-Ray crystallography. A detailed explanation of all the procedures followed for the preparation of the new **TTBrM** radical and **TTBrM-αH**, as well as all the reagents used for the given purpose, have been included in Section S1 of SI file. Moreover, further crystallographic data are also included in Section S2 of the SI file.

Chiral resolution. Racemic resolution was carried out on an Agilent 1260 series equipped with the following modules: quaternary pump (G7111B 1260 Quat Pump), automatic sample injector (G2258A 1260 DL ALS), column thermostat (G1316A 1260 TCC), DAD detector (G7115A 1260 DADWR) and an automatic sample collector (G1364C 1260 FC-AS). CHIRALPAK® IC packed with cellulose tris-(3,5-dichlorophenylcarbamate) immobilized on silica gel (5µm) was used as analytical column. The column temperature was set at 20 °C and the flow was constant during operation (1 mL/min).

1D NOESY/EXSY 1H NMR. NMR experiments were performed in an Advance NMR Bruker spectrometer operating at 400.13 MHz for 1H and equipped with a BBFO probe head. All NMR data were acquired and processed using the TOPSPIN v3.6 software package. Aiming at the achievement of accurate values for the chemical exchange, different experimental conditions were considered: *(i)* temperatures ranging from 20 to110 °C (293 and 383 K, according to the probe's upper thermal limit operation, 400 K); *(ii)* solvents of diverse viscosity (i.e., [D6]DMSO and [D8] dioxane); and different mixing times (r_m) from 50 to 1000 ms.

Chiroptical spectroscopies. ECD and CPL measurements were carried out with an Olis DSM172 spectrophotometer, equipped with a 150 W xenon lamp. The spectra were recorded in ~10^{-4} M in CCl_4 at -18 ºC. For ECD measurements, a fixed slit width of 1 mm and an integration time of

0.5 s were used. For CPL measurements, deoxygenated solutions were used, fixed slits of 3 and 3.16 mm, an excitation wavelength of 400 nm with a 150 W xenon lamp and an integration time of 1 s were selected. The final CPL spectra were acquired with a 1 point/nm resolution and averaged from 100 scans (around 135 s/scan). Significant contributions of linear polarization or optical artefacts were ruled out, and circular polarization was confirmed by observing the signal at a frequency of 2 × 50 kHz, 50 kHz being the frequency of the piezoelastic modulator (PEM) acting as an oscillating quarter-wave plate in our equipment.[37]

Time-Dependent Density-Functional Theory (TD-DFT) calculations. The ECD spectrum was calculated at the minimum energy geometry computed at the DFT UB3LYP/6-311+G** level of theory implemented in the Gaussian 09 program package.[38] Harmonic frequencies were computed to verify that the found stationary points were true minima. TD-DFT was employed to describe electronic transitions at the same level of theory. A correction of -0.25 eV was applied to the calculated ECD spectrum and a bandwidth of 0.25 eV was applied.

Acknowledgements

The authors are grateful for the financial support received from: MOTHER project (MAT2016-80826-R) granted by the DGI (Spain), GenCat (2017-SGR-918) financed by DGR (Catalunya) and the Spanish Ministry of Economy and Competitiveness (PGC2018-095808-B-I00 and PGC2018-101181-B-I00 projects) and through the “Severo Ochoa” Programme for Centres of Excellence in R&D (SEV-2015-0496) and through the “Proyecto Interdisciplinar de Frontera“, FIP-2018 HECTIC-PTM. We acknowledge the European Research Council (ERC) under the European Union’s Horizon 2020 research and innovation program (ERC-2015-STG-677023). This study has been also supported by the Networking Research Center on Bioengineering, Biomaterials and Nanomedicine (CIBER-BBN), an initiative funded by the VI National R&D&I Plan 2008-2011, Iniciativa Ingenio 2010, Consolider Program, CIBER Actions and financed by the Instituto de Salud Carlos III with assistance from the European Regional Development Fund. P. M. B. gratefully acknowledges financial support from the Juan de la Cierva-Formación 2015 programme (FJCI-2015-23577) supported by MINECO and, together with J.V, A. G. C. also thanks RyC-2013-12943 contract from MINECO. We also thankthe Servei de Ressonància Magnètica Nuclear, Universitat Autònoma de Barcelona, for allocating instrument time to this project.

Keywords: Circularly polarized luminescence • trityl radical • bromine substituents • racemization barrier •

[1] A. Obolda, X. Ai, M. Zhang, F. Li, *ACS Appl. Mater. Interfaces* **2016**, *8*, 35472-35478.

[2] Q. Peng, A. Obolda, M. Zhang, F. Li, *Angew. Chemie - Int. Ed.* **2015**, *54*, 7091-7095.

[3] M. Ballester, *Acc. Chem. Res.* **1985**, *18*, 380-387.

[4] D. Blasi, D. M. Nikolaidou, F. Terenziani, I. Ratera, J. Veciana, *Phys. Chem. Chem. Phys.* **2017**, *19*, 9313-9319.

[5] L. Fajarí, R. Papoular, M. Reig, E. Brillas, J. L. Jorda, O. Vallcorba, J. Rius, D. Velasco, L. Juliá, *J. Org. Chem.* **2014**, *79*, 1771-1777.

[6] A. Heckmann, S. Du, J. Pauli, M. Margraf, J. Ko, D. Stich, C. Lambert, I. Fischer, U. Resch-genger, C. Ro, *J. Phys. Chem. c* **2009**, *113*, 20958-20966.

[7] M. Souto, J. Calbo, I. Ratera, E. Ortí, J. Veciana, *Chem. Eur. J.* **2017**, *23*, 11067-11075.

[8] X. Wu, J. O. Kim, S. Medina, F. J. Ramírez, P. M. Burrezo, S. Wu, Z. L. Lim, C. Lambert, J. Casado, D. Kim, et al., *Chem. Eur. J.* **2017**, DOI 10.1002/chem.201701875.

[9] Y. Hattori, T. Kusamoto, H. Nishihara, *Angew. Chemie - Int. Ed.* **2014**, *53*, 11845-11848.

[10] Y. Hattori, T. Kusamoto, H. Nishihara, *Angew. Chemie - Int. Ed.* **2015**, *54*, 3731-3734.

[11] Y. Hattori, T. Kusamoto, T. Sato, H. Nishihara, *Chem. Commun.* **2016**, *52*, 13393-13396.

[12] T. Kusamoto, S. Kimura, Y. Ogino, C. Ohde, H. Nishihara, *Chem. Eur. J.* **2016**, *22*, 17725-17733.

[13] S. Kimura, A. Tanushi, T. Kusamoto, S. Kochi, T. Sato, H. Nishihara, *Chem. Sci.* **2018**, *9*, 1996-2007.

[14] S. Castellanos, D. Velasco, F. López-Calahorra, E. Brillas, L. Julia, *J. Org. Chem.* **2008**, *73*, 3759-3767.

[15] Y. Gao, W. Xu, H. Ma, A. Obolda, W. Yan, S. Dong, M. Zhang, F. Li, *Chem. Mater.* **2017**, *29*, 6733-6739.

[16] X. Ai, E. W. Evans, S. Dong, A. J. Gillett, H. Guo, Y. Chen, T. J. H. Hele, R. H. Friend, F. Li, *Nature* **2018**, *563*, 536-540.

[17] P. Mayorga Burrezo, V. G. Jiménez, D. Blasi, I. Ratera, A. G. Campaña, J. Veciana, *Angew. Chemie Int. Ed.* **2019**, *58*, 16282-16288.

[18] O. Armet, J. Veciana, C. Rovira, J. Riera, J. Castaner, E. Molins, J. Rius, C. Miravitlles, S. Olivella, J. Brichfeus, *J. Phys. Chem.* **1987**, *91*, 5608-5616.

[19] M. Ballester, J. Riera-Figueras, J. Castaner, C. Badfa, J. M. Monso, *J. Am. Chem. Soc.* **1971**, *93*, 2215-2225.

[20] K. Mislow, *Acc. Chem. Res.* **1976**, *9*, 26-33.

[21] E. L. Wehry, *Modern Fluorescence Spectroscopy*, Springer US, **1981**.

[22] H. Tanaka, Y. Inoue, T. Mori, *ChemPhotoChem* **2018**, *2*,

386-402.

[23] R. Filler, A. E. Fiebig, B. K. Mandal, *J. Fluor. Chem.* **2000**, *102*, 185–188.

[24] C. Trapp, C. Wang, R. Filler, *J. Chem. Phys.* **1966**, *45*, 3472-3474.

[25] M. Ballester, *Pure Appl. Chem.* **1967**, *15*, 123-152.

[26] S. R. Ruberu, M. A. Fox, *J. Phys. Chem.* **1993**, *97*, 143-149.

[27] I. Ratera, J. Veciana, *Chem. Soc. Rev.* **2012**, *41*, 303-349.

[28] Y. Hattori, T. Kusamoto, H. Nishihara, *RSC Adv.* **2015**, *5*, 64802-64805.

[29] R. S. Cahn, C. Ingold, V. Prelog, *Angew. Chemie Int. Ed. English* **1966**, *5*, 385-415.

[30] K. J. Weiland, T. Brandl, K. Atz, A. Prescimone, D. Häussinger, T. Šolomek, M. Mayor, *J. Am. Chem. Soc.* **2019**, *141*, 2104-2110.

[31] V. M. Tormyshev, A. M. Genaev, G. E. Sal'nikov, O. Y. Rogozhnikova, T. I. Troitskaya, D. V. Trukhin, V. I. Mamatyuk, D. S. Fadeev, H. J. Halpern, *European J. Org. Chem.* **2012**, *2012*, 623-629.

[32] C. M. Cruz, I. R. Márquez, I. F. A. Mariz, V. Blanco, C. Sánchez-Sánchez, J. M. Sobrado, J. A. Martín-Gago, J. M. Cuerva, E. Maçôas, A. G. Campaña, *Chem. Sci.* **2018**, *9*, 3917-3924.

[33] F. Furche, R. Ahlrichs, C. Wachsmann, E. Weber, A. Sobanski, F. Vögtle, S. Grimme, *J. Am. Chem. Soc.* **2000**, *122*, 1717-1724.

[34] I. Warnke, F. Furche, *Wiley Interdiscip. Rev. Comput. Mol. Sci.* **2012**, *2*, 150-166.

[35] E. M. Sánchez-Carnerero, A. R. Agarrabeitia, F. Moreno, B. L. Maroto, G. Muller, M. J. Ortiz, S. de la Moya, *Chem. Eur. J.* **2015**, *21*, 13488-13500.

[36] D. Blasi, D. M. Nikolaidou, F. Terenziani, I. Ratera, J. Veciana, *Phys. Chem. Chem. Phys.* **2017**, *19*, 9313-9319.

[37] H. P. J. M. Dekkers, P. F. Moraal, J. M. Timper, J. P. Riehl, *Appl. Spectrosc.* **1985**, *39*, 818-821.

[38] M. Frisch, G. Trucks, H. Schlegel, G. Scuseria, *Gaussian, Inc., Wallingford, CT* **2009**.

Entry for the Table of Contents

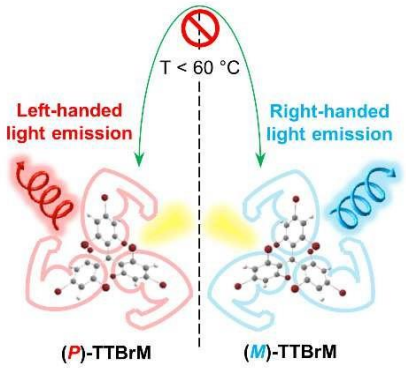

An efficient circularly polarized luminescence emitter, based on a persistent trityl radical substituted with bulky bromine atoms at *ortho*- and *para*-positions. Additionally, a high racemization barrier between its enantiomers is reported.

Institute and/or researcher Twitter usernames: @icmabCSIC; @NanomolGroup; @Campana_Lab